


Please cite the Published Version

Souza, Maria MC, Rocha, Raquel G, Siqueira, Gilvana P, Crapnell, Robert D, Richter, Eduardo M, Banks, Craig E  and Muñoz, Rodrigo AA (2025) Additively manufactured ready-to-use platform using conductive recycled PLA for ketamine sensing. *Mikrochimica acta*, 192 (2). p. 60. ISSN 0026-3672

DOI: <https://doi.org/10.1007/s00604-024-06902-3>

Publisher: Springer Science and Business Media LLC

Version: Accepted Version

Downloaded from: <https://e-space.mmu.ac.uk/638026/>

Usage rights:  [Creative Commons: Attribution 4.0](https://creativecommons.org/licenses/by/4.0/)

Additional Information: This is an author-produced version of the published paper. Uploaded in accordance with the University's Research Publications Policy

Data Access Statement: Data available upon request from the authors.

Enquiries:

If you have questions about this document, contact openresearch@mmu.ac.uk. Please include the URL of the record in e-space. If you believe that your, or a third party's rights have been compromised through this document please see our Take Down policy (available from <https://www.mmu.ac.uk/library/using-the-library/policies-and-guidelines>)

Additively manufactured ready-to-use platform using conductive recycled PLA for ketamine sensing

Maria M. C. Souza¹ · Raquel G. Rocha¹ · Gilvana P. Siqueira¹ · Robert D. Crapnell² · Eduardo M. Richter¹ · Craig E. Banks² · Rodrigo A. A. Muñoz¹

Abstract

The use of 3D-printed electrodes is reported fabricated from in-house conductive filament composed of a mixture of recycled poly (lactic acid) (rPLA), graphite (Gpt), and carbon black (CB) for fast detection of the abused drug ketamine. Firstly, the performance of these electrodes was evaluated in comparison to 3D-printed electrodes produced employing a commercially available conductive filament. After a simple pretreatment step (mechanical polishing), the new 3D-printed electrodes presented better performance than the electrodes produced from commercial filament in relation to peak-to-peak separation of the redox probe $[\text{Fe}(\text{CN})_6]^{3-/4-}$ (130 mV and 759 mV, respectively), charge transfer resistance ($R_{ct} = 1.04 \pm 0.05 \text{ k}\Omega$ and $9.62 \pm 0.03 \text{ k}\Omega$, respectively), and heterogeneous rate constant ($k^0 = 7.16 \pm 0.05 \times 10^{-3} \text{ cm s}^{-1}$ and $3.57 \pm 0.03 \times 10^{-3} \text{ cm s}^{-1}$, respectively). Excellent analytical characteristics for the detection of ketamine were achieved, including wide linear range (10 to $250 \mu\text{mol L}^{-1}$), excellent sensitivity ($0.024 \pm 0.001 \mu\text{A } \mu\text{mol L}^{-1}$), low limit of detection (LOD = $0.7 \mu\text{mol L}^{-1}$), and recovery values from 82 to 115% for beverage samples (white and red wines, beer, water, and vodka) spiked with the abused drug ketamine.

Keywords 3D printing · Disposable device · Drugs of abuse · Electrochemical sensor · Differential pulse voltammetry · Beverage samples · Date rape drug · Circular economy

Introduction

The use of drugs of abuse is a significant global issue [1]. In 2019, the United Nations Office on Drugs and Crime (UNODC) estimated that approximately 35 million people suffered from substance use disorders, with around half a million deaths attributed to drug overdoses each year [2]. Many drugs, commonly known as “date rape drugs,” are used to facilitate sexual assault, where the victim—either voluntarily or unknowingly—consumes a substance that impairs their ability to give consent, leading to non-consensual sexual activity [3]. Therefore, the accurate quantification of the prevalence of date rape drugs is challenging,

as victims, predominantly women, often present amnesia or choose not to report the assault due to fear of victim-blaming [1].

Despite of this, the European Monitoring Centre for Drugs and Drug Addiction reports that 75% of rape victims were drugged with illicit substances, alcohol, or a combination of both [4]. This statistic highlights the need for increased awareness and action to prevent drug-facilitated sexual violence. The substances used include common drugs: alcohol (ethanol), benzodiazepines (midazolam, flunitrazepam, diazepam, etc.), antihistamines (diphenhydramine and hydroxyzine), ketamine (KET), barbiturates (phenobarbital, secobarbital, thiopental, etc.), gamma-hydroxybutyric acid (GHB), opioids (fentanyl, morphine, etc.) and other less popular drugs, including emerging recreational drugs [5, 6]; however, the most common drugs applied as date rape drug are ethanol, benzodiazepines, GHB and KET [6].

KET, also known as Cat Valium, Kitkat, and Super K, is a common dissociative anesthetic medication used in surgical procedures for both humans and animals as it

✉ Rodrigo A. A. Muñoz
munoz@ufu.br

¹ Federal University of Uberlândia, Chemistry Institute, Uberlândia, MG 38400-902, Brazil

² Faculty of Science and Engineering, Manchester Metropolitan University, Dalton Building, Chester Street, Manchester, Great Britain M1 5GD, UK

can cause a loss of consciousness. Its use for recreational purposes started in 1971 and, in the 1980s, KET usage became more prevalent in drug-facilitated sexual assaults. The incidence of KET abuse was reported at 1.7% in the UK in 2008/2009, and around 1% among American college students [7]. Moreover, there has been a noted increase in overdose cases linked with KET consumption [8]. It is important to emphasize that KET is odorless and tasteless, meaning it does not alter the flavor of the victim's drink, hence its prevalence in sexual assault cases. Recently, U.S. Food and Drug Administration (FDA) also approved the use of KET as an antidepressant [7, 9, 10].

From a forensic point of view, screening tests must be reliable, whilst enabling rapid and on-site detection of substances [11, 12]. Usually, colorimetric tests are employed for this purpose, and although these tests are rapid and low-cost, they offer lower selectivity and rely on subjective interpretations [13, 14]. In this context, electrochemical methods offer advantageous characteristics, such as minimal sample handling, high sensitivity, cost-effectiveness, rapidity, selectivity, and easy miniaturization. Recently, Balamurugan and co-workers reviewed current trends in the development of electrochemical sensors aimed at the detection of date rape drugs [15].

In recent years, interest in 3D-printing technology, particularly in Fused Filament Fabrication (FFF), has surged due to its notable advantages, such as the following: (i) the ability to produce mass-scale and custom-designed objects; (ii) reduced waste generation compared to traditional subtractive manufacturing methods; (iii) cost-effective production; and (iv) a broad and continuously expanding range of printable materials [16, 17]. Some research groups have been exploring the potential applications of 3D-printed electrodes for detecting various target substances in forensic samples, including cocaine [18], atropine [19], explosives [20], and amphetamine-type substances [21]. Commercially available filaments, composed of poly(lactic acid) (PLA) as the polymer and carbon black (CB) as the conductive filler, have been utilized for constructing additively manufactured electrodes (AMEs). However, a growing trend in 3D-printing electrochemistry is the development of custom-made filaments [22]. This approach aims to enhance sustainability and reduce production costs [23]. Additionally, the use of plasticizers allows for the incorporation of higher amounts of conductive materials while maintaining the filament's flexibility, which significantly increase the electrochemical performance of the sensor compared to commercially available CB/PLA electrodes [22, 23].

Plastic waste has garnered significant attention in recent years as a critical environmental challenge [24–26]. The concept of a circular economy has emerged as the most promising alternative solution to address plastic pollution. In 2015, European Union proposed a “Plastics in a circular

economy” that consisted of an action plan and proposals for revised legislation on waste [27]. This is an interesting contribution of the European Union to develop a sustainable, low carbon, resource efficient and competitive economy. A circular economy encompasses strategies, practices, policies, and technologies aimed at achieving principles such as reusing, recycling, redesigning, repurposing, remanufacturing, refurbishing, and recovering water, waste materials, and nutrients to preserve natural resources [28]. This approach creates essential conditions to motivate economic and social interested parties to adopt sustainability-oriented strategies. Recently, Sigley and co-workers introduced the idea of circular economy in electrochemistry field [28]. For this purpose, the authors used recycled PLA from post-industrial coffee pod waste to construct electrochemical cell as well as additive manufactured electrodes for detecting caffeine.

Moreover, Cruvinel and colleagues demonstrated the production of a filament based on graphite (12 wt %), carbon black (18 wt %), as conductive materials, and castor oil (10 wt %) and recycled PLA (60 wt %) as a bioplasticizer and thermoplastic material, respectively, for the detection of TNT residues in simulated explosions [29]. Importantly, the electrochemical device required only surface polishing before use to obtain a smooth surface, which is a remarkable advantage compared to most 3D-printed electrodes that necessitate additional surface treatment protocols [30]. Herein, we proposed the construction of AMEs using FFF technology to detect KET in spiked beverage samples (vodka, red wine, beer, white wine and drinking water). A conductive filament made from recycled PLA, incorporating carbon black and graphite, and castor oil, was used to produce working electrodes.

Experimental

Chemical and samples

All standard reagents were analytical grade and employed without further purification. Deionized water with a resistivity greater than 18 M Ω cm (Millipore Direct-Q3 water purification, MA, USA) was used to prepare all aqueous solutions. KET was donated by the Civil Police of Minas Gerais (Belo Horizonte, Brazil). Potassium chloride ($\geq 99.5\%$ w/w) was purchased from Êxodo Científica (São Paulo, Brazil), potassium ferricyanide (99% w/w) from Labsynth (Diadema, Brazil), hexaammineruthenium trichloride (98% w/w) and atropine sulfate (pharmaceutical secondary standard) from Sigma Aldrich (St. Louis, USA), acetic and phosphoric acids from Vetec (Rio de Janeiro, Brazil), boric acid (99% w/w) from AppliChem Panreac (Barcelona, Spain), sodium hydroxide (98%

w/w) from ChemiFlex (São Bernardo do Campo, Brazil). Cocaine and benzodiazepines (midazolam, clonazepam, diazepam, and bromazepam) were donated by the Brazilian Federal Police (Minas Gerais, Brazil).

Phosphoric, acetic and boric acids, all in 0.04 mol L⁻¹, were used in the preparation of Britton-Robinson buffer (BR). The pH values of BR solutions were subsequently adjusted with the addition of 1 mol L⁻¹ NaOH prior use as supporting electrolyte.

Sample preparation

Beverage samples (red and white wines, beer, drinking water, and vodka) were acquired from local supermarkets (Uberlândia, Brazil). These samples were spiked with a 5 mmol L⁻¹ KET, diluted in supporting electrolyte (200 times) and analyzed using the standard addition method.

Filament production

The filament production was conducted following established protocols in the literature [29]. Before use, the recycled polylactic acid (rPLA) was dried (60 °C/ 2.5 h) to eliminate any residual water. The filament composition comprised 65 wt % rPLA, 10 wt % castor oil, 18 wt % CB, and 12 wt % graphite, which were mixed at 70 rpm with a Thermo Haake Polydrive Dynameter equipped with a Thermo Haake Rheomix 600 (Thermo, Germany) at 190 °C for 5 min. The polymer composites were collected and processed through the hopper of a EX6 extrusion line (Filabot, VA, United States). The EX6 was set up with a single screw with four set heat zones of 60, 190, 195, and 195 °C, respectively. The molten polymer was extruded from a 1.75 mm die head, pulled along an Airpath cooling line (Filabot, VA, United States) and collected on a spool. After which the filament was then ready to use for additive manufacturing, as described in previous work [31].

Construction of 3D-printed working electrodes

The additive manufactured working electrode (AME) was printed using a Flash Forge Dreamer NX (São José dos Campos, São Paulo, Brazil) equipped with 0.8 mm nozzle at 220 °C with a bed temperature of 90 °C. Briefly, a square shaped electrode (1 cm × 1 cm) was produced with the following printing parameters: layer thickness of 0.18 mm, two perimeters in a horizontal orientation with 100% infill density and a constant printing speed of 70 mm s⁻¹. The 3D-printing parameters were selected based on previous works using the same filament [29]. The electrochemical cell (internal volume = 10 mL, Figure S1) was printed using acrylonitrile butadiene styrene (ABS) filament (GTMax, São

Paulo, Brazil) and a GTMax 3D printer (São Paulo, Brazil). More information about it, is described by Cardoso et al. [32]. In this 3D-printed cell, the working electrode area was always defined by rubber O-rings with the same internal diameter (i.d. = 5 mm cm; 0.22 cm²).

Characterization

Electrochemical measurements

Cyclic voltammetry (CV), differential pulse voltammetry (DPV), and electrochemical impedance spectroscopy (EIS) measurements were carried out in the presence of dissolved oxygen and at room temperature, using a potentiostat/galvanostat PGSTAT108N (Metrohm Autolab BV, Utrecht, The Netherlands). The NOVA 2.1.7 software were used to acquire and processing data (baseline correction for DPV scans). A platinum wire and lab-made Ag|AgCl with saturated KCl solution were employed as auxiliary and reference electrodes, respectively. AMEs constructed with recycled PLA (rPLA), graphite and carbon black (Gpt-CB-rPLA) was used as working electrodes. In order to compare the electrochemical activity of the proposed Gpt-CB-rPLA, 3D-printed electrodes were also fabricated using a commercial conductive filament based on carbon black and PLA (CB-PLA; Protopasta®, WA, USA).

EIS data were obtained using an open circuit potential (+0.22 V vs. Ag|AgCl|KCl_(sat.)) in the presence of 2 mmol L⁻¹ [Fe(CN)₆]^{3-/4-} and 0.1 mol L⁻¹ KCl solution, with an application of an alternating potential of 10 mV amplitude over a frequency range from 30 kHz to 0.1 Hz. The equivalent Randles circuit was used to fit the experimental data and to determine the charge transfer resistance (R_{ct}) related to the [Fe(CN)₆]^{3-/4-} species.

Results and discussion

Characterization

The lab-made conductive filament (Gpt-CB-rPLA) presented excellent flexibility at room temperature, as observed in Fig. 1A. Moreover, the proposed filament demonstrated good printability since the construction of square-shaped AMEs was possible. Although the filament is flexible for ease of printing, the produced working electrode does not exhibit the same flexibility, being less flexible compared to the filament. The SEM image of the filament revealed an irregular pattern with the presence of flake-like structures attributed to the graphite inserted in the composite (Fig. 1B). This non-uniform texture is typical of thermoplastic composites and contributes to more surface interactions.

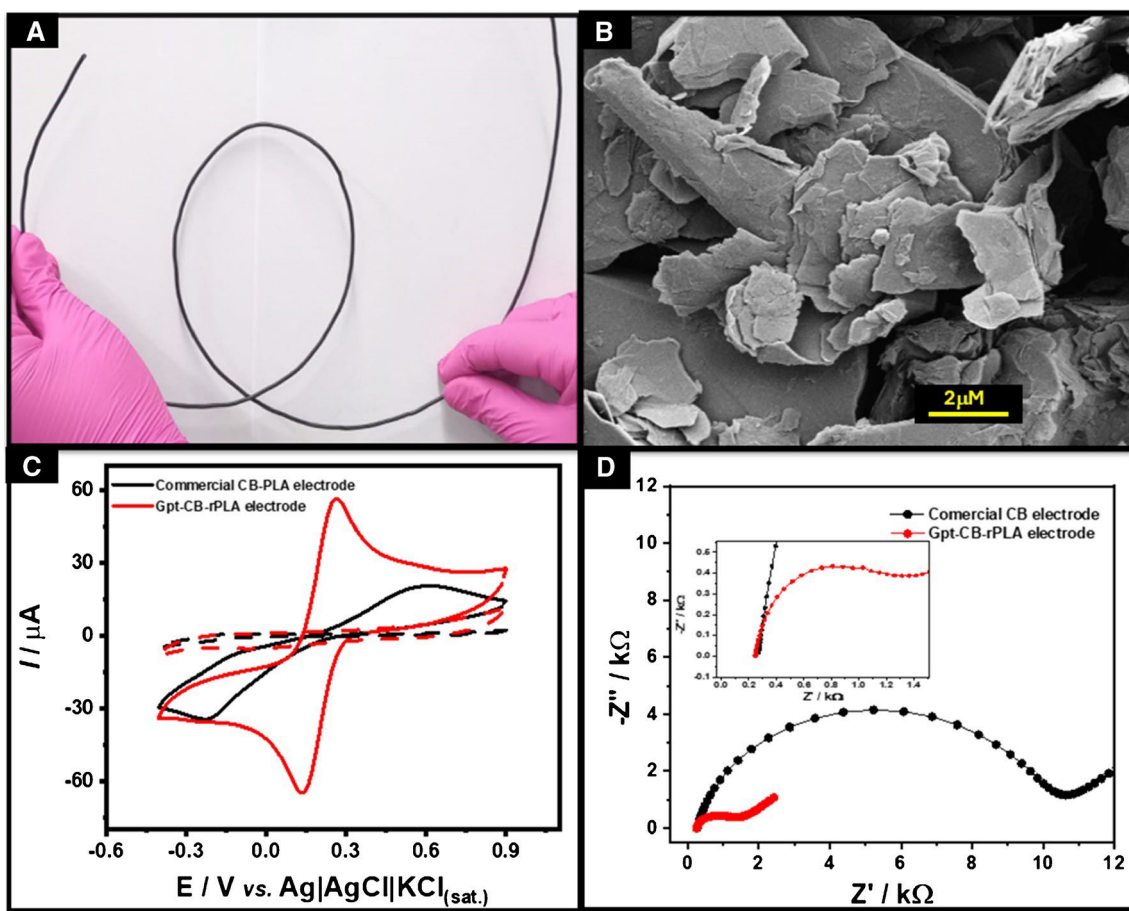


Fig. 1 **A** Real image of the lab-made filament; **(B)** SEM image of Gpt-CB-rPLA electrode surface; **(C)** Cyclic voltammograms recorded at 1 mmol L⁻¹ [Fe(CN)₆]^{3-/4-} in 0.1 mol L⁻¹ KCl solution and the dashed lines refer the blank of analysis. CV conditions: scan rate at 50 mV s⁻¹ and step potential (5 mV) and **(D)** Nyquist

plots recorded in the presence of 1.0 mmol L⁻¹ [Fe(CN)₆]^{3-/4-} in 0.1 mol L⁻¹ KCl solution applying a half-wave potential (+0.22 V vs. Ag|AgCl|KCl_(sat.)), using commercial CB-PLA (black line) and Gpt-CB-rPLA (red line) electrodes. Solid line refers the fitting line

To better understand the results, the electrochemical activity of the Gpt-CB-rPLA electrode was compared with AMEs constructed from commercially conductive CB-PLA filament using cyclic voltammetry (50 mV s⁻¹). A summary of the results from all electrochemical characterizations are shown in Table 1, emphasizing the peak anodic current (I_{pa}) and the peak-to-peak separation (ΔE_p) obtained for the near-ideal outer-sphere ([Ru(NH₃)₆]^{2+/3+}, Figure S1) and commonly used inner-sphere ([Fe(CN)₆]^{3-/4-}, Fig. 1C) probes

(both 1 mmol L⁻¹ in KCl 0.1 mol L⁻¹). As observed in Figure S2, the Gpt-CB-rPLA electrode showed a better electrochemical response for the outer-sphere probe. However, this effect is more pronounced when using an inner-sphere probe, where an ill-defined voltammetric profile was achieved at CB-PLA electrodes, along with a higher peak-to-peak separation (ΔE_p > 750 mV compared to 130 mV). Moreover,

Table 1 Comparison of some electrochemical parameters obtained for commercial CB-PLA and Gpt-CB-rPLA working electrodes

Parameters	Commercial CB-PLA	Gpt-CB-rPLA
^a ΔE _p / mV	75 ± 1	67 ± 1
^a I _{pa} / μA	12.6 ± 0.9	19.5 ± 0.7
^b ΔE _p / mV	759 ± 3	130 ± 3
^b I _{pa} / μA	20.5 ± 1.0	56.4 ± 0.7
^c k ⁰ × 10 ⁻³ / cm s ⁻¹	3.57 ± 0.03	7.16 ± 0.05
^b R _{ct} / kΩ	9.62 ± 0.03	1.04 ± 0.05

Data extracted from cyclic voltammetry at 50 mVs⁻¹ in the presence of ^aouter-sphere ([Ru(NH₃)₆]^{3+/2+}) and ^binner-sphere ([Fe(CN)₆]^{3-/4-}) probe, both 1.0 mmol L⁻¹, using 0.1 mol L⁻¹ KCl solution as supporting electrolyte. ^ck⁰ was estimated using CVs scan rates studies (20–100 mV s⁻¹) in the presence of 1 mmol L⁻¹ [Ru(NH₃)₆]^{3+/2+} in 0.1 mol L⁻¹ KCl solution

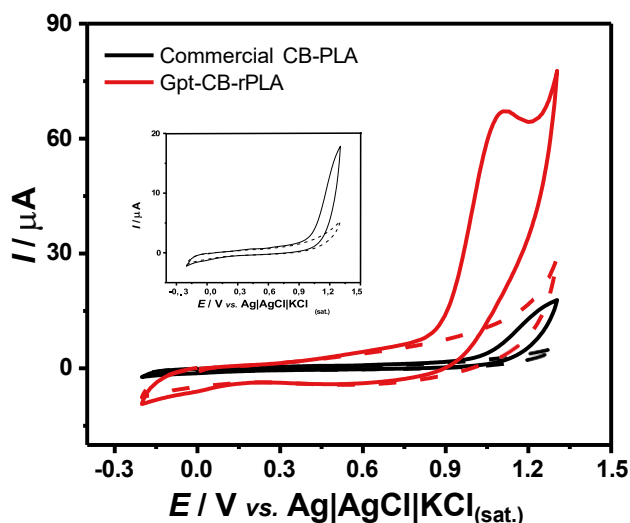


Fig. 2 Cyclic voltammograms obtained without (dashed lines) and with (solid lines) the presence of 1 mmol L⁻¹ KET in 0.12 mol L⁻¹ BR buffer (pH = 9.0) with 0.1 mol L⁻¹ KCl at Gpt-CB-rPLA (red line) and CB-PLA (black line) electrodes. CVs conditions: scan rate (50 mV s⁻¹) and step potential (5 mV)

CVs of 1.0 mmol L⁻¹ [Fe(CN)₆]^{3-/4-} in Fig. 1C also indicates 2.8-fold increase in the anodic peak current when using Gpt-CB-rPLA electrodes. Next, data from scan rate studies (20–100 mV s⁻¹) were plotted to determine the heterogeneous electrochemical rate constant (k^0) in the presence of 1.0 mmol L⁻¹ [Ru(NH₃)₆]^{2+/3+} in a 0.1 mol L⁻¹ KCl solution (Figure S3 in Supplementary Information). The calculated k^0 values were $(3.57 \pm 0.03) \times 10^{-3}$ and $(7.16 \pm 0.05) \times 10^{-3}$ cm s⁻¹ for CB-PLA and Gpt-CB-rPLA electrodes, respectively. These findings further demonstrate the enhanced electrochemical

activity of the newly conductive filament to construct AMEs. Moreover, the Rct values estimated from EIS plots of Fig. 1D ($R_{ct} = 1.04 \pm 0.05$ and 9.62 ± 0.03 k Ω for Gpt-CB-rPLA and CB-PLA) corroborate these results described above.

Electrochemical determination of KET in beverage samples

Preliminary CV experiments were carried out to understand the electrochemical behavior of KET, using both electrodes (Fig. 2) in 0.12 mol L⁻¹ BR buffer (pH = 9.0). An ill-defined oxidation peak was observed using the commercial CB-PLA electrode (inset of Fig. 2), whereas an irreversible oxidation process occurred at around +1.1 V (vs. Ag|AgCl|KCl_(sat.)) in the presence of 1.0 mmol L⁻¹ KET for the Gpt-CB-rPLA AME. Interestingly, the Gpt-CB-rPLA electrode produced a significantly enhanced voltammogram over the commercial CB-PLA, as evidenced by the shift to less positive peak potentials and notable increase in current intensity. This result, once again, agreed with the previous studies mentioned above, involving the inner-sphere probe. In fact, the presence of the plasticizer in the proposed conductive filament allows for the incorporation of a higher amount of conductive filler, which contributes to enhancing the electrochemical activity of the AMEs [22].

In the next step, the effect of pH on the electrochemical behavior of KET was assessed using 0.12 mol L⁻¹ BR buffer at different pH values (2.0–12.0) with the Gpt-CB-rPLA material as the working electrode, shown in Fig. 3. The peak related to the oxidation of the secondary amine in the KET structure was observed in the pH range of 7 to 12. At pH values below 7.0, no signals were detected (data not shown) within the evaluated potential window (0.0

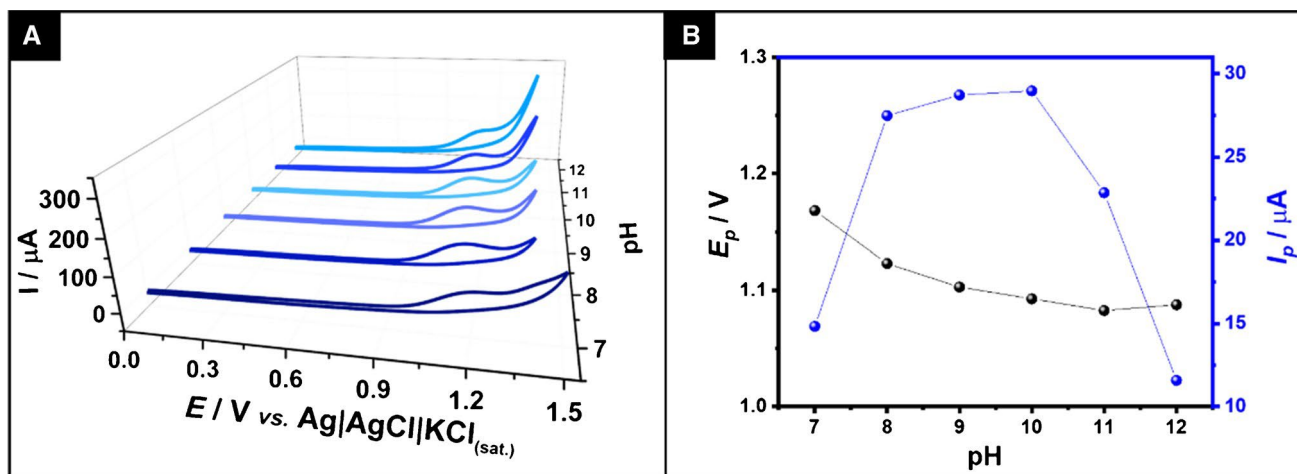


Fig. 3 (A) Effect of pH (7.0 to 12.0) on CV responses for 1.0 mmol L⁻¹ KET in 0.12 mol L⁻¹ BR buffer with 0.1 mol L⁻¹ KCl using the Gpt-CB-rPLA as the working electrode, and (B) the relationship

between peak potentials (E_p) and peak currents (I_p) with pHs. CV conditions: scan rate (50 mV s⁻¹) and step potential (5 mV)

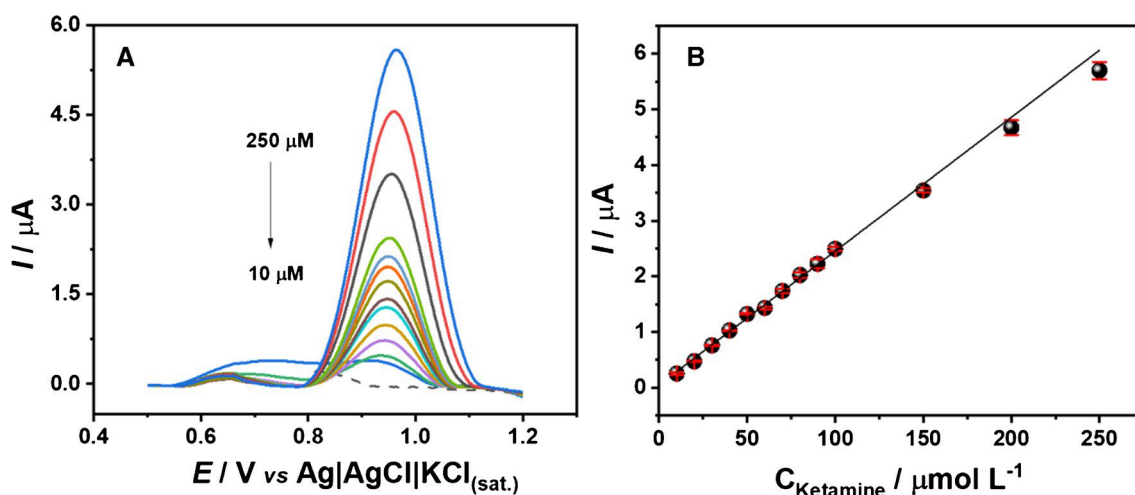


Fig. 4 (A) Baseline-corrected DPV recorded for increasing KET concentrations (10 to 250 $\mu\text{mol L}^{-1}$) in 0.12 mol L^{-1} BR buffer (pH = 9.0) with 0.1 mol L^{-1} KCl and the (B) respective calibration

plot. DPV conditions: step potential of 4 mV, amplitude of 80 mV and modulation time of 40 ms

to +1.5 V vs. Ag|AgCl|KCl_(sat.)), which is consistent with literature reports [33]. In acidic medium, the secondary amine group of KET is protonated ($\text{pK}_a = 7.5$), resulting in a higher energy barrier for the electrochemical oxidation. The highest peak current was observed at pH 9.0, which was selected for further studies.

A differential pulse voltammetric (DPV) measurement was used to demonstrate the potential applicability of AMEs fabricated from Gpt-CB-rPLA filament for KET determination. The DPV parameters (modulation amplitude, step potential and modulation time) were systematically optimized (univariate test), as shown in Figures S4, S5 and S6, with the best results obtained using a step potential of 4 mV, modulation time of 40 ms and amplitude of 80 mV. Afterward, these optimized DPV parameters were used to obtain the calibration curve for KET determination. Figure 4 shows that the oxidation peak current increased linearly ($R^2 = 0.994$) in the concentration range between 10.0 and 250.0 $\mu\text{mol L}^{-1}$, following the equation: $I_p(\mu\text{A}) = (0.024 \pm 0.001) C_{\text{KET}}(\mu\text{mol L}^{-1}) + (0.049 \pm 0.028)$. Additional information is highlighted in Table 2. A wide linear range was achieved, demonstrating the potential of Gpt-CB-rPLA electrodes for the detection of KET in forensic samples. The limit of detection (LOD) was determined in accordance with IUPAC guidelines ($\text{LOD} = 3\sigma/s$), where σ is the standard deviation of blank signals ($n = 10$) and s is the sensitivity (slope) of the analytical curve. The estimated LOD value (0.7 $\mu\text{mol L}^{-1}$) is appropriate to detect KET in forensic samples. For example, the average sedative dose is around

0.75 mg kg^{-1} [34]. Thus, for individuals weighing 65 kg, the concentration in a drink is around 49 mg per 100 mL

average sedative dose [35, 36], the doses associated with KET abuse are often significantly higher. Reports indicate that recreational doses of KET typically range from 100 to 200 mg [8, 35]. These elevated doses raise concerns regarding the potential risk of overdose associated with recreational use.

The inter-electrode reproducibility of Gpt-CB-rPLA was investigated ($n = 5$), and the results are presented in Figure S7 (C and D). The scans were performed with 50 $\mu\text{mol L}^{-1}$ of ketamine on each electrode. The results showed high precision between the electrodes, with a relative standard deviation (RSD) of 3.2%. Repeatability studies ($n = 10$) were also evaluated, using the same electrode throughout the day to determine 50 $\mu\text{mol L}^{-1}$ of ketamine (Figure S7 A and B), obtaining an RSD value of 3.6%, confirming the precision of the filament used.

As proof of the concept, various beverage samples (drinking water, beer, white and red wines and vodka) were spiked

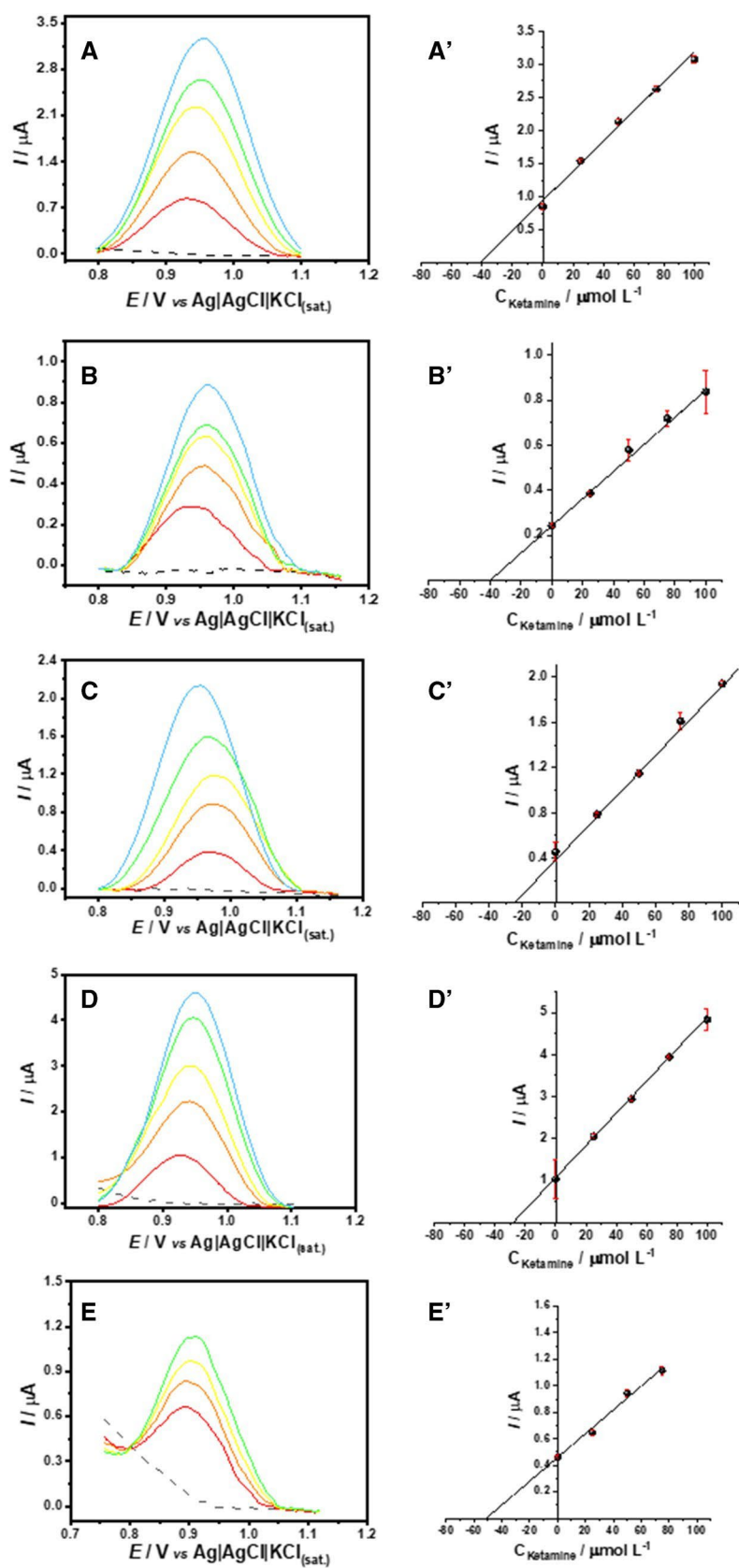
Table 2 Results of some analytical parameters obtained for KET detection using 3D-printed Gpt-CB-rPLA as the working electrode

Analytical Parameters	Gpt-CB-rPLA
R^2	0.994
Linear range ($\mu\text{mol L}^{-1}$)	10 to 250
Slope ($\mu\text{A}\mu\text{mol L}^{-1}$)	0.024 ± 0.001
Intercept (μA)	0.049 ± 0.028
LOD ($\mu\text{mol L}^{-1}$)	0.7
LOQ ($\mu\text{mol L}^{-1}$)	2.2
RSD (inter-electrode, $n = 5$, 50 $\mu\text{mol L}^{-1}$) / %	3.2
RSD (intra-electrode, $n = 10$, 50 $\mu\text{mol L}^{-1}$) / %	3.6

(2 mmol L⁻¹). Although the median lethal dose (LD₅₀) of KET in humans is estimated to be 100-times higher than the

*R*²: coefficient of determination; *LOD*: limit of detection; *LOQ*: limit of quantification; *RSD*: relative standard deviation

Fig. 5 Baseline-corrected DPV responses for spiked beverage samples (A) vodka, (B) beer, (C) red wine, (D) white wine, and (E) drinking water diluted (200-fold) in 0.12 mol L⁻¹ BR buffer solution with 0.1 mol L⁻¹ KCl (pH = 9.0) with successive additions of increasing concentrations of KET. The dashed lines refer the beverage samples diluted in the supporting electrolyte without KET. DPV conditions: see Fig. 4



with a specific concentration of KET, diluted in supporting electrolyte, and analyzed using the standard addition method (Fig. 5). As observed, no analytical signals were detected near the KET peak position for any of the beverage samples (dashed line in Fig. 5). As noted in Table 3, satisfactory recovery values (82–115%) attested that the proposed method displayed good accuracy and is free from interference of beverage sample matrices.

Interfering species

As previously reported, some species, including clonazepam (CZP), bromazepam (BZP), diazepam (DZP), midazolam (MDZ), and atropine (ATR), have been used as date rape drugs [15]. In this context, studies were conducted to assess whether these compounds could potentially interfere with the detection and identification of KET. The electrochemical response using DPV scans of all interfering species and KET, both in $200 \mu\text{mol L}^{-1}$, were compared under optimized conditions. As can be noticed in Figure S8, it is evident that midazolam and diazepam did not exhibit peaks corresponding to the KET position, indicating a clear separation between KET and the this examined compounds. However, CZP, ATR and BZP can interfere in the electrochemical response. In this sense, a study of $50 \mu\text{mol L}^{-1}$ KET in the presence of these potential interfering species was also conducted (Figure S9) with the interfering ratio in 1:1 or 2:1. Although atropine in higher concentration ($200 \mu\text{mol L}^{-1}$ for both compounds in Figure S8) seems to present a slight interference on KET peak position, in the evaluated ratio, atropine does not affect significantly the KET signal. Indeed, a decrease in the KET peak current occurs with the addition of different concentrations of bromazepam and clonazepam. However, these effects can be solved using the standard addition method, which can overcome sample matrix effects.

Table 3 A summary of results obtained for KET determination in spiked beverage samples analyzed by DPV using the standard addition method and the Gpt-CB-rPLA electrode

Sample	Spiked ($\mu\text{mol L}^{-1}$)	Recovery ($\mu\text{mol L}^{-1}$)	Recovery (%)
Vodka (A)	50	42 ± 1	83 ± 1
Beer (B)	50	41 ± 4	82 ± 8
Red wine (C)	25	24 ± 3	99 ± 1
White wine (D)	25	28 ± 1	115 ± 1
Drinking water (E)	50	51 ± 3	103 ± 5

Comparison of the proposed method with other electrochemical procedures reported for KET detection

Finally, the analytical parameters (linear range and limit of detection) of the proposed method were compared to those from other electrochemical methods previously reported for KET determination (Table S2). As observed, the Gpt-CB-rPLA sensor exhibited superior analytical performance than screen printed carbon electrodes [33, 37] or carbon paste electrodes [38]. Despite some studies reporting superior analytical parameters [39–43], most of the methods in the literature rely on working electrodes that require labor-intensive and expensive modification processes. Additionally, Liu and Wang reported a biosensor for KET detection in biological samples; however, the use of biological modifications requires controlled conditions and can complicate the sensor's stability and reproducibility [41]. It is important to mention that 3D printing technology is a powerful apparatus to develop electroanalytical devices designed for the detection of KET in different sample types. While many AMEs reported in the literature require post-treatment to improve electrochemical activity, the Gpt-CB-rPLA composite does not need any additional activation to boost its electrochemical performance.

Conclusion

This study demonstrated that a laboratory-developed conductive filament comprising graphite, carbon black, and recycled PLA (Gpt-CB-rPLA) can be effectively utilized for the fabrication of AMEs specifically tailored for KET detection. AMEs constructed with the laboratory-made conductive filament (Gpt-CB-rPLA) exhibited superior electrochemical performance (smaller peak-to-peak separation and higher current intensity for an inner-sphere probe) compared to those produced using the commercial CB/PLA filament. Moreover, the Gpt-CB-rPLA sensor exhibited lower charge transfer resistance and higher heterogeneous electron transfer rate constant (k^0). Additionally, the material cost for 1 kg of the Gpt-CB-rPLA mixture is £59, significantly lower than the commercial £107 required for the commercial filament. This cost efficiency is primarily

attributed to the fact that graphite powder is approximately twelve times less expensive than carbon black. This material was subsequently used for the electrochemical detection of KET in spiked beverage samples, yielding a sensitivity of $0.024 \pm 0.001 \mu\text{A } \mu\text{mol L}^{-1}$ and a LOD of $0.7 \mu\text{mol L}^{-1}$. Moreover, the 3D-printed Gpt-CB-rPLA sensor was tested

for the detection of KET within a spiked beverage sample, achieving recovery rates between 82 and 115%. This research underscores the potential of the 3D printing technology to produce electrodes with excellent electrochemical performance while offering a more sustainable and cost-effective approaches (use of recycled PLA).

Author contribution MMCS, RGR and GSP wrote the first version of the manuscript and performed most of the experiments presented. RDC synthesized and characterized the conductive filaments. RDC, EMR, CEB and RAAM corrected the final version of the manuscript. CEB, EMR and RAAM provided resources and funding. RAAM was responsible for supervision and project administration. All authors reviewed the manuscript.

Funding The authors are thankful to the Brazilian science foundation agencies CNPq (grants 405620/2021-7, 308392/2022-1, 408462/2022-1, 409680/21-4, 401977/2023-4, 315838/2021-3, and 406958/2022-0 INCT-SP), FAPEMIG (grants APQ-02067-23, RED-00120-23, and APQ-02391-22), and CAPES (financial code 001) for financial support.

References

1. Kuehn BM (2012) WHO Documents Worldwide Need for Better Drug Abuse Treatment—and Access to It. *JAMA* 308:442. <https://doi.org/10.1001/jama.2012.8882>
2. Canton H (2021) United Nations Office on Drugs and Crime—UNODC. The Europa Directory of International Organizations 2021. Routledge, London, pp 240–244
3. Frison G, Favretto D, Tedeschi L, Ferrara SD (2003) Detection of thiopental and pentobarbital in head and pubic hair in a case of drug-facilitated sexual assault. *Forensic Sci Int* 133:171–174. [https://doi.org/10.1016/S0379-0738\(03\)00064-1](https://doi.org/10.1016/S0379-0738(03)00064-1)
4. Olszewski D (2009) Sexual assaults facilitated by drugs or alcohol. *Drugs: Education, Prevention and Policy* 16:39–52. <https://doi.org/10.1080/09687630802128756>
5. Scott-Ham M, Burton FC (2005) Toxicological findings in cases of alleged drug-facilitated sexual assault in the United Kingdom over a 3-year period. *J Clin Forensic Med* 12:175–186. <https://doi.org/10.1016/j.jcfm.2005.03.009>
6. Sonone SS, Jadhav S, Sankhla MS (2021) A forensic aspect on drug facilitated sexual assault. *Forensic Res Crim Int J* 9:59–63. <https://doi.org/10.15406/frcij.2021.09.00341>
7. DeWilde KE, Levitch CF, Murrough JW et al (2015) The promise of ketamine for treatment-resistant depression: current evidence and future directions. *Ann N Y Acad Sci* 1345:47–58. <https://doi.org/10.1111/nyas.12646>
8. Sinner B, Graf BM (2008) Ketamine. In: *Modern anesthetics*. Springer Berlin Heidelberg, Heidelberg, pp 313–333. https://doi.org/10.1007/978-3-540-74806-9_15
9. Anzar N, Suleman S, Parvez S, Narang J (2022) A review on Illicit drugs and biosensing advances for its rapid detection. *Process Biochem* 113:113–124. <https://doi.org/10.1016/j.procbio.2021.12.021>
10. Krystal JH, Kavalali ET, Monteggia LM (2024) Ketamine and rapid antidepressant action: new treatments and novel synaptic signaling mechanisms. *Neuropharmacology* 49:41–50. <https://doi.org/10.1038/s41386-023-01629-w>
11. Fakayode SO, Brady PN, Grant C et al (2024) Electrochemical Sensors, Biosensors, and Optical Sensors for the Detection of Opioids and Their Analogs: Pharmaceutical, Clinical, and Forensic Applications. *Chemosensors* 12:58. <https://doi.org/10.3390/chemosensors12040058>
12. Murugan B, Mahalingam U, Ramasamy P, Sagadevan S (2024) Nanomaterial functionalized electrode for forensic electrochemistry for the sensing of psychoactive compounds, pp 151–185. <https://doi.org/10.1021/bk-2024-1481.ch007>
13. Philp M, Fu S (2018) A review of chemical ‘spot’ tests: A presumptive illicit drug identification technique. *Drug Test Anal* 10:95–108. <https://doi.org/10.1002/dta.2300>
14. Kranenburg RF, Ramaker H, van Asten AC (2022) On-site forensic analysis of colored seized materials: Detection of brown heroin and MDMA-tablets by a portable NIR spectrometer. *Drug Test Anal* 14:1762–1772. <https://doi.org/10.1002/dta.3356>
15. Balamurugan TST, Kwaczyński K, Rizwan M, Poltorak L (2024) Current trends in rapid electroanalytical screening of date rape drugs in beverages. *TrAC, Trends Anal Chem* 175:117712. <https://doi.org/10.1016/j.trac.2024.117712>
16. Solomon IJ, Sevel P, Gunasekaran J (2021) A review on the various processing parameters in FDM. *Mater Today Proc* 37:509–514. <https://doi.org/10.1016/j.matpr.2020.05.484>
17. Abdalla A, Patel BA (2021) 3D Printed electrochemical sensors. *Annu Rev Anal Chem* 14:47–63. <https://doi.org/10.1146/annurev-anchem-091120-093659>
18. Rocha RG, Ribeiro JS, Santana MHP et al (2021) 3D-printing for forensic chemistry: voltammetric determination of cocaine on additively manufactured graphene–polylactic acid electrodes. *Anal Methods* 13:1788–1794. <https://doi.org/10.1039/D1AY0181G>
19. Arantes IVS, Crapnell RD, Whittingham MJ et al (2023) Additive manufacturing of a portable electrochemical sensor with a recycled conductive filament for the detection of atropine in spiked drink samples. *ACS Appl Eng Mater* 1:2397–2406. <https://doi.org/10.1021/acsaem.3c00345>
20. Tan C, Nasir MZM, Ambrosi A, Pumera M (2017) 3D Printed electrodes for detection of nitroaromatic explosives and nerve agents. *Anal Chem* 89:8995–9001. <https://doi.org/10.1021/acs.analchem.7b01614>
21. de Faria LV, Macedo AA, Arantes LC et al (2024) Novel disposable and portable 3D-printed electrochemical apparatus for fast and selective screening of 25E-NBOH in forensic samples. *Talanta* 269:125476. <https://doi.org/10.1016/j.talanta.2023.125476>
22. Crapnell RD, Kalinke C, Silva LRG et al (2023) Additive manufacturing electrochemistry: An overview of producing bespoke conductive additive manufacturing filaments. *Mater Today* 71:73–90. <https://doi.org/10.1016/j.mattod.2023.11.002>

-
23. Kalinke C, Crapnell RD, de Oliveira PR et al (2024) How to Improve Sustainability in Fused Filament Fabrication (3D Printing) Research? *Global Challenges* 8:2300408. <https://doi.org/10.1002/gch2.202300408>
 24. Syberg K, Nielsen MB, Westergaard Clausen LP et al (2021) Regulation of plastic from a circular economy perspective. *Curr Opin Green Sustain Chem* 29:100462. <https://doi.org/10.1016/j.cogsc.2021.100462>
 25. Singh S, Chunglok W (2022) Potential application of biopolymers as biodegradable plastic. In: *Biopolymers Towards Green and Sustainable Development*. Bentham Science Publishers, pp 139–152. <https://doi.org/10.2174/9789815079302122010009>
 26. Hahladakis JN, Iacovidou E, Gerassimidou S (2020) Plastic waste in a circular economy. In: *Plastic Waste and Recycling*. Elsevier, pp 481–512. <https://doi.org/10.1016/B978-0-12-817880-5.00019-0>
 27. European Commission Plastics in a circular economy. In: https://research-and-innovation.ec.europa.eu/research-area/environment/circular-economy/plastics-circular-economy_en
 28. Sigley E, Kalinke C, Crapnell RD et al (2023) Circular Economy Electrochemistry: Creating Additive Manufacturing Feedstocks for Caffeine Detection from Post-Industrial Coffee Pod Waste. *ACS Sustain Chem Eng* 11:2978–2988. <https://doi.org/10.1021/acssuschemeng.2c06514>
 29. Souza MC, Siqueira P, Rocha G et al (2025) Additively manufactured collector-detector device for explosive analysis using recycled PLA filament loaded with carbon black and graphite. *J Braz Chem Soc* 36:e-20240186. <https://doi.org/10.21577/0103-5053.20240186>
 30. Rocha DP, Rocha RG, Castro SVF et al (2022) Posttreatment of 3D-printed surfaces for electrochemical applications: A critical review on proposed protocols. *Electrochem Sci Adv* 2:e2100136. <https://doi.org/10.1002/elsa.202100136>
 31. Crapnell RD, Arantes IVS, Whittingham MJ et al (2023) Utilising bio-based plasticiser castor oil and recycled PLA for the production of conductive additive manufacturing feedstock and detection of bisphenol A. *Green Chem* 25:5591–5600. <https://doi.org/10.1039/D3GC01700A>
 32. Cardoso RM, Mendonça DMH, Silva WP et al (2018) 3D printing for electroanalysis: From multiuse electrochemical cells to sensors. *Anal Chim Acta* 1033:49–57. <https://doi.org/10.1016/j.aca.2018.06.021>
 33. Schram J, Parrilla M, Slegers N et al (2020) Identifying electrochemical fingerprints of ketamine with voltammetry and liquid chromatography-mass spectrometry for its detection in seized samples. *Anal Chem* 92:13485–13492. <https://doi.org/10.1021/acs.analchem.0c02810>
 34. Newton A, Fitton L (2008) Intravenous ketamine for adult procedural sedation in the emergency department: a prospective cohort study. *Emerg Med J* 25:498–501. <https://doi.org/10.1136/emj.2007.053421>
 35. Sassano-Higgins S, Baron D, Juarez G et al (2016) A review of ketamine abuse and diversion. *Depress Anxiety* 33:718–727. <https://doi.org/10.1002/da.22536>
 36. Wolff K, Winstock AR (2006) Ketamine. *CNS Drugs* 20:199–218. <https://doi.org/10.2165/00023210-200620030-00003>
 37. Stelmaszczyk P, Białkowska K, Sekuła K et al (2024) Screen-printed electrode-based sensor for rapid ketamine determination: optimization and on-site application for seized drugs analysis. *Monatshfte für Chemie - Chem Monthly* 155:881–888. <https://doi.org/10.1007/s00706-024-03237-w>
 38. Abu Shawish HM, Saadeh SM, Tamos H et al (2015) A new potentiometric sensor for the determination of ketamine hydrochloride in ampoules and urine. *Anal Methods* 7:301–308. <https://doi.org/10.1039/C4AY01986E>
 39. Asghary M, Raoof JB, Ojani R, Hamidi-Asl E (2015) A genosensor based on CPE for study the interaction between ketamine as an anesthesia drug with DNA. *Int J Biol Macromol* 80:512–519. <https://doi.org/10.1016/j.ijbiomac.2015.07.019>
 40. Bagheryan Z, Raoof J, Ojani R, Hamidi-Asl E (2013) Introduction of ketamine as a g-quadruplex-binding ligand using platinum nanoparticle modified carbon paste electrode. *Electroanalysis* 25:2659–2667. <https://doi.org/10.1002/elan.201300418>
 41. Liu L, Wang P (2024) Fabrication of an electrochemical impedance sensor for ketamine hydrochloride and its application in the detection of doping substances in sports. *Int J Electrochem Sci* 19:100520. <https://doi.org/10.1016/j.ijoes.2024.100520>
 42. Deiminiat B, Rounaghi GH (2018) Fabrication of a new electrochemical imprinted sensor for determination of ketamine based on modified polytyramine/sol-gel/f-MWCNTs@AuNPs nanocomposite/pencil graphite electrode. *Sens Actuators B Chem* 259:133–141. <https://doi.org/10.1016/j.snb.2017.12.062>
 43. Jin C, Li M, Duan S et al (2023) An electrochemical sensor for direct and sensitive detection of ketamine. *Biosens Bioelectron* 226:115134. <https://doi.org/10.1016/j.bios.2023.115134>